

Insight into the Scalar Mesons from a Lattice Calculation

Mark Alford and R. L. Jaffe

*Center for Theoretical Physics,
Laboratory for Nuclear Science and Department of Physics,
Massachusetts Institute of Technology,
Cambridge, Massachusetts 02139*

Abstract

We study the possibility that the light scalar mesons are $\bar{q}^2 q^2$ states rather than $\bar{q}q$. We perform a lattice QCD calculation of pseudoscalar meson scattering amplitudes, ignoring quark loops and quark annihilation, and find indications that for sufficiently heavy quarks there is a stable four-quark bound state with $J^{PC} = 0^{++}$ and non-exotic flavor quantum numbers.

I. INTRODUCTION

The light scalar mesons have defied classification for decades [1,2]. Some are narrow and have been firmly established since the 1960's. Others are so broad that their very existence is controversial. Scalar mesons are predicted to be chiral partners of the pseudoscalars like the pion, but their role in chiral dynamics remains obscure. Naive quark models interpret them as orbitally excited $\bar{q}q$ states. Others have suggested that they are \bar{q}^2q^2 [3] or “molecular” states, [4] strongly coupled to $\pi\pi$ and $\bar{K}K$ thresholds.

In this paper we propose a way to shed some light on the nature of the scalar mesons using lattice QCD. Previously scalar mesons have been treated like other mesons: their masses have been extracted from the large Euclidean time falloff of $\bar{q}q - \bar{q}q$ correlation functions with the appropriate quantum numbers. Here we look for a 0^{++} \bar{q}^2q^2 *bound state*. We construct \bar{q}^2q^2 sources, work in the quenched approximation, and discard $\bar{q}q$ annihilation diagrams so communication with $\bar{q}q$ and vacuum channels is forbidden. Also, we allow the quark masses to be large (hundreds of MeV), so the continuum threshold for the decay $\bar{q}^2q^2 \rightarrow (\bar{q}q)(\bar{q}q)$ is artificially elevated. We then study the large Euclidean time falloff of a $\bar{q}^2q^2 - \bar{q}^2q^2$ correlator, looking for a falloff slower than $2m_{\bar{q}q}$, signalling a bound state. Such an object would have been missed by studies of $\bar{q}q$ correlators in the quenched approximation. We use shortcomings of lattice QCD to our advantage. By excluding processes that mix $\bar{q}q$ and \bar{q}^2q^2 , we can unambiguously assign a quark content to a state. The heavy quark mass suppresses relativistic effects, which we believe complicate the interpretation of light quark states.

Our initial results are encouraging: within the limits of our computation we see signs of a bound state in the “non-exotic” \bar{q}^2q^2 channel, namely, the one with quantum numbers that could also characterize a $\bar{q}q$ state ($I = 0$ for 2 flavors, the **1** and **8** for 3 flavors). In contrast, the “exotic” flavor \bar{q}^2q^2 channel ($I = 2$ for 2 flavors, the **27** for 3 flavors) shows no bound state. Instead it shows a negative scattering length, characteristic of a repulsive interaction. To obtain a definitive result will require larger lattices and more computer time, but this is well within the scope of existing facilities.

In Sec. II we give an overview of the 0^{++} mesons. First we summarize the phenomenology. Then we summarize previous lattice calculations. We also review earlier studies of \bar{q}^2q^2 sources on the lattice. [5,6] Because these earlier works looked only at one (relatively small) lattice size they were unable to examine the possibility of a bound state. In Sec. III we summarize our computation. First we briefly review \bar{q}^2q^2 operators and discuss lattice size and quark mass dependence. Next, we review the improved lattice action we use to enable us to study larger lattices. [7] Finally in Sec. IV we present our results and discuss their implications. We explore some of the directions in which our computation could be improved.

A reader who wishes to skip the details can look immediately at Fig. 5 where we plot the dependence on lattice size of the binding energy associated with the exotic and non-exotic \bar{q}^2q^2 channels. The exotic channel shows a negative binding energy with the $1/L^3$ dependence expected from analysis of the $(\bar{q}q)(\bar{q}q)$ continuum. [8] The coefficient of $1/L^3$ agrees roughly with Refs. [5,6] and with the predictions of chiral perturbation theory. The non-exotic channel shows positive binding energy, but seems to depart from $1/L^3$, perhaps approaching a constant as $L \rightarrow \infty$, which would indicate the existence of a bound \bar{q}^2q^2 state. Confirmation of this result will require further calculations on larger lattices.

II. OVERVIEW OF THE LIGHT SCALAR MESONS

In this section we establish the context for our work. First we give a very brief introduction to the phenomenology of the lightest 0^{++} mesons composed of light (u , d , and s) quarks. We give a sketch of the $\bar{q}q$ and \bar{q}^2q^2 models for 0^{++} states and contrast them. More information can be found in Refs. [1,2] and references quoted therein. Next we summarize existing lattice calculations which relate to the 0^{++} channel. These fall into two classes: traditional searches for $\bar{q}q$ eigenstates and attempts to learn about low energy $\pi\pi$ scattering by studying \bar{q}^2q^2 sources.

A. Phenomenology

The known 0^{++} mesons divide into effects near and below 1 GeV, which are unusual, and effects in the 1.3–1.5 GeV region which may be more conventional. Here we focus on the states below 1 GeV. Altogether, the objects below 1 GeV form an $SU(3)_f$ nonet: two isosinglets, an isotriplet and two strange isodoublets. The isotriplet and one isosinglet are narrow and well confirmed. The isodoublets and the other isosinglet are very broad and still controversial.

The well established 0^{++} mesons are the isosinglet $f_0(980)$ and the isotriplet $a_0(980)$. Both are relatively narrow: $\Gamma[f_0] \sim 40$ MeV, $\Gamma[a_0] \sim 50$ MeV,¹ despite the presence of open channels ($\pi\pi$ for the f_0 and $\pi\eta$ for the a_0) for allowed s-wave decays. Both couple strongly to $\bar{K}K$ and lie so close to the $\bar{K}K$ threshold at 987 MeV that their shapes are strongly distorted by threshold effects. Interpretation of the f_0 and a_0 requires a coupled channel scattering analysis. The relevant channels are $\pi\pi$ and $\bar{K}K$ for the f_0 and $\pi\eta$ and $\bar{K}K$ for the a_0 . In both cases the results favor an intrinsically broad state, strongly coupled to $\bar{K}K$ and weakly coupled to the other channel. The physical object appears narrow because the $\bar{K}K$ channel is closed over a significant portion of the object's width. No summary this brief does justice to the wealth of work and opinion in this complex situation.

The other light scalar mesons are known as broad enhancements in very low energy s-wave meson-meson scattering. The enhancements are universally accepted, but their interpretation is more controversial. At the lowest energies only the $\pi\pi$ channel is open. The $\pi\pi$ s-wave can couple either to isospin zero or two. The $I = 2$ (e.g. $\pi^+\pi^+$) channel shows a weak repulsion in rough agreement with the predictions of chiral low energy theorems. [9] The $I = 0$ channel shows a strong attraction: the phase shift rises steadily from threshold to approximately $\pi/2$ by ~ 800 MeV before effects associated with the f_0 complicate the picture. This low mass enhancement in the $\pi\pi$ s-wave is the σ meson of nuclear physics and chiral dynamics. Recent studies support the existence of an S-matrix pole associated with this state at a mass around 600 MeV, which we will refer to as the $\sigma(600)$. [2,10] The πK s-wave is very similar to $\pi\pi$. The exotic $I = 3/2$ (e.g. π^+K^+) channel shows weak repulsion. The non-exotic $I = 1/2$ channel shows relatively strong attraction. Black et al. [2] identify

¹We use the observed peak width into $\pi\pi$ and $\pi\eta$ respectively, rather than some more model dependent method for extracting a width.

the enhancement with an S-matrix pole at approximately 900 MeV, which is known as the $\kappa(900)$. The enhancement is not in doubt, but the interpretation is, if anything, more controversial than the $\pi\pi$ case.² Other couplings of these objects (the σ can couple to $\bar{K}K$ and the κ can couple to ηK) are unknown because the relevant thresholds lie above the states. The large widths of these states reflect their strong coupling to the open decay channels $\pi\pi$ and πK respectively.

The conventional quark model assigns the 0^{++} mesons to the first orbitally excited multiplet of $\bar{q}q$ states. As in positronium, 0^{++} quantum numbers are made by coupling $L = 1$ to $S = 1$ to give total $J = 0$. The 0^{++} states should be very similar to the $1^{+\pm}$ and 2^{++} $\bar{q}q$ states that lie in the same family. These are very well known and form conventional meson nonets (in $SU(3)_f$). Since they have a unit of excitation (orbital angular momentum), they are expected to be quite a bit heavier than the pseudoscalar and vector mesons. Most models put the $\bar{q}q$ 0^{++} mesons along with their 2^{++} and 1^{++} brethren around 1.2–1.5 GeV.

An idealized $\bar{q}q$ meson nonet has a characteristic pattern of masses and decay couplings. The vector mesons are best known, but the pattern is equally apparent in the 2^{++} or 1^{++} nonets. The isotriplet and the isosinglet composed of non-strange quarks are lightest and are roughly degenerate (e.g. the ρ and the ω). The strange isodoublets are heavier because they contain a single strange quark (e.g. the K^*). The final isosinglet is heaviest because it contains an $\bar{s}s$ pair (e.g. the ϕ). Decay patterns show selection rules which follow from this quark content. In particular, the lone isosinglet does not couple to non-strange mesons ($\phi \not\rightarrow 3\pi$). The mass pattern, quark content and natural decay couplings of a $\bar{q}q$ nonet are summarized in Fig. 1a. These patterns seem to bear little resemblance to the masses and couplings of the light 0^{++} mesons, a fact which led earlier workers to explore other interpretations.

Four quarks ($\bar{q}^2 q^2$) can couple to 0^{++} without a unit of orbital excitation. Furthermore, the color and spin dependent interactions, which arise from one gluon exchange, favor states in which quarks and antiquarks are separately antisymmetrized in flavor. For quarks in 3-flavor QCD the antisymmetric state is the flavor $\bar{\mathbf{3}}$. Thus the energetically favored configuration for $\bar{q}^2 q^2$ in flavor is $(\bar{q}\bar{q})^{\bar{\mathbf{3}}}(qq)^{\mathbf{3}}$, a flavor nonet. The lightest multiplet has spin 0. Explicit studies in the MIT Bag Model indicated that the color-spin interaction could drive the $\bar{q}^2 q^2$ 0^{++} nonet down to very low energies: 600 to 1000 MeV depending on the strangeness content. [3]

The most striking feature of a $\bar{q}^2 q^2$ nonet in comparison with a $\bar{q}q$ nonet is an *inverted mass spectrum* (see Fig. 1b). The crucial ingredient is the presence of a hidden $\bar{s}s$ pair in several states. The flavor content of $(qq)^{\mathbf{3}}$ is $\{[ud], [us], [ds]\}$, where the brackets denote antisymmetry. When combined with $(\bar{q}\bar{q})^{\bar{\mathbf{3}}}$, four of the resulting states contain a hidden $\bar{s}s$ pair: the isotriplet and one of the isosinglets have quark content $\{u\bar{d}s\bar{s}, \frac{1}{\sqrt{2}}(u\bar{u} - d\bar{d})s\bar{s}, d\bar{u}s\bar{s}\}$ and $\frac{1}{\sqrt{2}}(u\bar{u} + d\bar{d})s\bar{s}$, and therefore lie at the top of the multiplet. The other isosinglet, $u\bar{d}\bar{d}u$ is the only state without strange quarks and therefore lies alone at the bottom of the multiplet. The strange isodoublets ($u\bar{s}d\bar{d}$, etc.) should lie in between. In summary, one expects a degenerate isosinglet and isotriplet at the top of the multiplet and strongly coupled to $\bar{K}K$, an isosinglet at the bottom, strongly coupled to $\pi\pi$, and a strange isodoublet coupled to $K\pi$

²For example, the $\kappa(900)$ is not mentioned in Ref. [1]

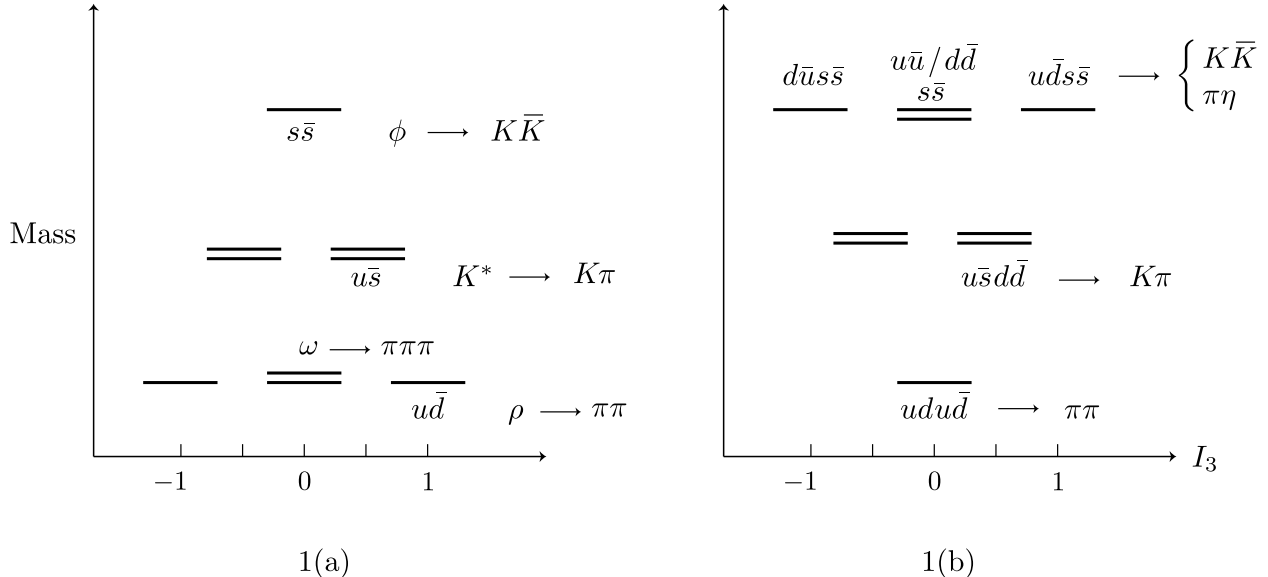


FIG. 1. The mass pattern, quark content and natural decay couplings of (a) a $\bar{q}q$ nonet and (b) a \bar{q}^2q^2 nonet.

in between (Fig. 1b). The resemblance to the observed structure of the light 0^{++} states is considerable.

These qualitative considerations motivate a careful look at the classification of the scalar mesons. Models of QCD are not sophisticated enough to settle the question. For example, the \bar{q}^2q^2 picture does not distinguish between one extreme where the four quarks sit in the lowest orbital of some mean field, [3] and the other, where the four quarks are correlated into two $\bar{q}q$ mesons which attract one another in the flavor $(\bar{q}\bar{q})^3(qq)^3$ channel. [11,4] For years, phenomenologists have attempted to analyse meson-meson scattering data in ways which might distinguish between $\bar{q}q$ and \bar{q}^2q^2 assignments. A recent quantitative study favors the \bar{q}^2q^2 assignment. [2] However the $\bar{q}q$ assignment has strong advocates. [10] We hope that a suitably constrained lattice calculation can aid in the eventual classification of these states.

B. Existing Lattice Studies

In this section we briefly summarize existing lattice calculations which bear on the classification of the 0^{++} mesons. There have been lattice studies of both the spectrum of 0^{++} states and the mixing of $\bar{q}q$ states with glueballs.

Unquenched spectroscopic calculations are just beginning to become available [12,13]. In principle, they are of interest because they would couple to a \bar{q}^2q^2 configuration if it is energetically favorable. One unquenched calculation reports tentative evidence of 0^{++} state at an energy much lower than that reported in quenched calculations [13]. We return to this work briefly in our conclusions. Further insight from unquenched calculations will have to await more definitive studies.

For the rest of this section, we restrict ourselves to consideration of quenched calculations. We will not discuss the mixing of glueballs with $\bar{q}q$ states, because we are interested in

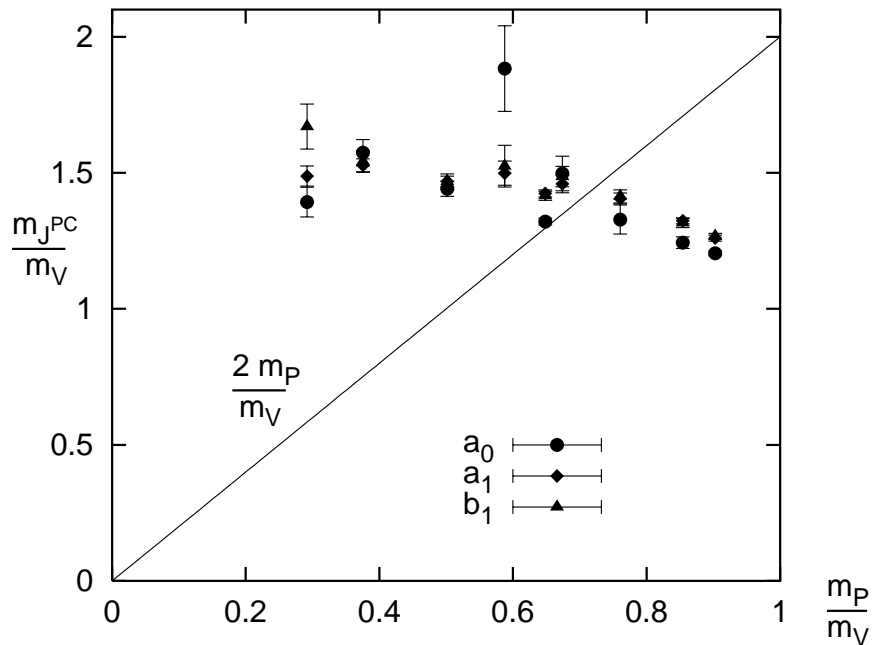


FIG. 2. Quenched lattice calculations [15,17] of the ratio of the masses of various p -wave $\bar{q}q$ mesons to the vector meson mass, as a function of the pseudoscalar to vector mass ratio, ie with varying quark mass. The threshold for decay to PP is also shown.

distinguishing $\bar{q}q$ from \bar{q}^2q^2 components of mesons. First we consider quenched studies of $\bar{q}q$ spectra. Then we describe attempts to extract meson-meson scattering lengths from quenched studies of \bar{q}^2q^2 sources.

1. $\bar{q}q$ Spectrum Calculations

The masses of the 0^{++} $\bar{q}q$ states have been calculated on the lattice in the quenched approximation by various groups [14–17]. Some of their results are shown in Fig. 2. As well as the $J^{PC} = 0^{++}(a_0)$, we have included data from the same groups on the other positive parity mesons $J^{PC} = 1^{++}(a_1)$ and $1^{+-}(b_1)$. Data for the $2^{++}(a_2)$ was not available. The spectra in Fig. 2 behave roughly as $\bar{q}q$ states with orbital angular momentum should. In the heavy quark limit, as the pseudoscalar mass m_P approaches the vector mass m_V , their masses approach one another because spin and spin-orbit splittings decrease with m_q , and approach m_V because orbital excitation energy decreases with m_q . To make this behavior manifest we plot $m_{J^{PC}}/m_V$ versus m_P/m_V , and note that $m_{J^{PC}}/m_V$ approaches unity as m_P/m_V increases.

2. Pseudoscalar Scattering Length Calculations

In the past, lattice studies of four-quark states have been undertaken in order to extract pseudoscalar-pseudoscalar (P - P) scattering lengths for comparison with the predictions of

chiral dynamics. It is known [8] that the energy shift δE of a two-particle state with quantum numbers α in a cubic box of size L is related to the threshold scattering amplitude,

$$\delta E_\alpha = E_\alpha - 2m_P = \frac{T_\alpha}{L^3} \left(1 + 2.8373 \frac{m_P T_\alpha}{4\pi L} + 6.3752 \left(\frac{m_P T_\alpha}{4\pi L} \right)^2 + \dots \right), \quad (1)$$

where m_P is the mass of the scattering particles, and T_α is the scattering amplitude at threshold in the channel labelled by α , which can be related to the scattering length,

$$T_\alpha = -\frac{4\pi a_\alpha}{m_P}. \quad (2)$$

For a more detailed discussion, see Ref. [18]. In our case the channels of interest are exotic ($I = 2$, for two flavors) and non-exotic ($I = 0$, for two flavors). If the interaction is attractive enough to produce a bound state, then instead of eq. (1) one would find that δE goes to a negative constant as $L \rightarrow \infty$.

In order to distinguish between a bound state and the continuum behavior described by eq. (1), it is necessary to perform calculations for several different lattice sizes. Calculations with $\bar{q}^2 q^2$ sources have been performed by Gupta et al. [5], who studied one lattice volume at one lattice spacing, and Fukugita et al. [6], who, for the heavy quark masses we are interested in, also studied only one lattice volume at one lattice spacing. Their results were therefore not sufficient to check the lattice-size dependence of energy of the two-pseudoscalar state, and investigate the possibility of a bound state. Our method follows theirs, but we have studied a range of lattice sizes. Their results are plotted along with ours in Fig. 5. Where our calculations overlap, they agree.

III. A $\bar{q}^2 q^2$ EXERCISE ON THE LATTICE

A. Quark contractions and flavor dependence

For our purposes the salient categorization of $\bar{q}^2 q^2$ correlators is into “exotic” channels (flavor states that are only possible for a $\bar{q}^2 q^2$ state, $I = 2$ for two flavors, the **27** for three flavors) and non-exotic channels (flavor states that could be $\bar{q}^2 q^2$ or $\bar{q}q$, $I = 0$ for two flavors, the **8** and **1** for three flavors). In the absence of quark annihilation diagrams, the **8** and **1** are identical. When annihilation is included, the **1**, like the $I = 0$ for two flavors, can mix with pure glue. As shown in Fig. 3, the $\bar{q}^2 q^2$ 0^{++} correlation functions can be expressed in terms of a basis determined by the four ways of contracting the quark propagators [18]: direct (D), crossed (C), single annihilation (A), complete annihilation into glue (G). Since we are interested in $\bar{q}^2 q^2$ states, we only study the D and C contributions. We will assume that all quarks are degenerate, so there is only one quark mass, and as far as color and spinor indices are concerned all quark propagators are the same. In our lattice calculation we will therefore build our $\bar{q}^2 q^2$ correlators from color and spinor traces of contractions of four identical quark propagators, putting in the flavor properties by hand when we choose the relative weights of the different contractions.

In the case of two flavors, there are two possible channels for a spatially symmetric source: $I = 2$ (exotic) and $I = 0$ (non-exotic). Evaluation of the flavor dependence of the quark line contractions shows that the $I = 2$ channel is $D - C$, and $I = 0$ is $D + \frac{1}{2}C$ [18].

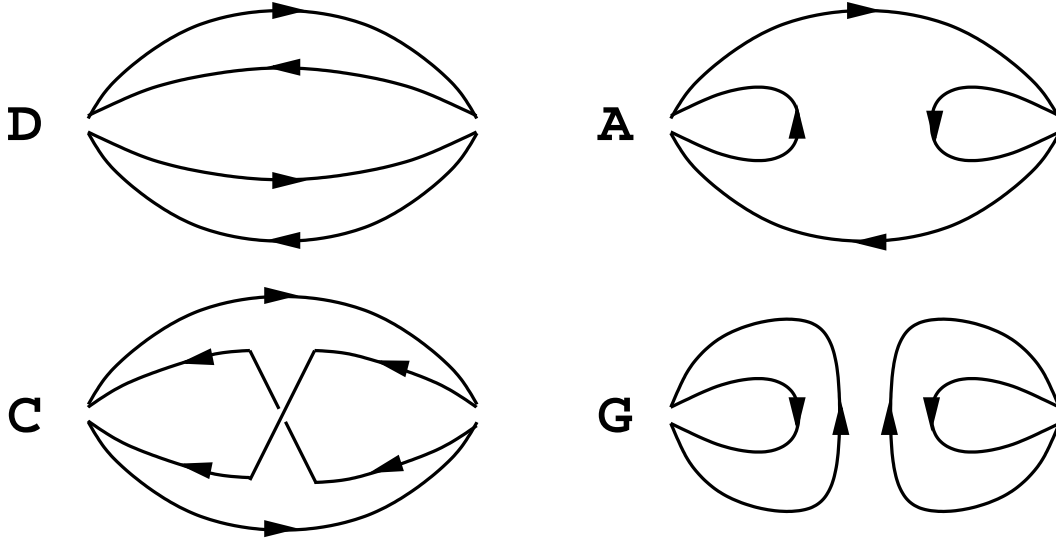


FIG. 3. The four types of quark line contraction that contribute to the pseudoscalar-pseudoscalar (P - P) correlation function.

For three flavors, the possible channels are the symmetric parts of $\mathbf{3} \times \mathbf{3} \times \bar{\mathbf{3}} \times \bar{\mathbf{3}}$, namely $\mathbf{1} + \mathbf{8}$ (non-exotic) and $\mathbf{27}$ (exotic). As in the two-flavor case, the exotic channel is $D - C$. At sufficiently large Euclidean time separation, each contraction will behave as a sum of exponentials, corresponding to the states it overlaps with. Generically, all linear combinations will be dominated by the same state: the lightest. Only with correctly chosen relative weightings will the leading exponential cancel out, yielding a faster-dropping exponential corresponding to a more massive state. We will see in Sec. IV that the exotic ($D - C$) channel is the one where such a cancellation occurs, yielding a repulsive interaction between the pseudoscalars. For *any* other linear combination of D and C the correlator is therefore dominated by the lightest, attractive state. Without loss of generality, we can therefore study the following linear combinations:

$$\begin{array}{llll}
 \text{Exotic:} & J_E = D - C & 2 \text{ flavor: } I = 2 & 3 \text{ flavor: } \mathbf{27} \\
 \text{Non-exotic:} & J_N = D + \frac{1}{2}C & 2 \text{ flavor: } I = 0 & 3 \text{ flavor: } \mathbf{1, 8}
 \end{array} \tag{3}$$

We conclude that if, as our results suggest, there is a bound $\bar{q}^2 q^2$ state in the non-exotic channel, then this means that with two flavors, the $I = 0$ channel is bound, and with three flavors both the $\mathbf{1}$ and $\mathbf{8}$ are bound. Once quark loops and annihilation diagrams are included, the $\mathbf{1}$ and $\mathbf{8}$ will split apart. Unquenched lattice calculations will be needed to see if they remain bound.

B. Lattice action

In our lattice calculations, we work in the quenched (valence) approximation, and use Symanzik-improved glue and quark actions. This means that irrelevant terms ($\mathcal{O}(a)$, $\mathcal{O}(a^2)$, where a is the lattice spacing) have been added to the lattice action to compensate for discretization errors.

Improved actions are crucial to our ability to explore a range of physical volumes using limited computer resources. Because most of the finite-lattice-spacing errors have been removed, we can use coarse lattices, which have fewer sites and hence require much less computational effort: note that the number of floating-point-operations required even for a quenched lattice QCD calculation rises faster than a^{-4} .

Improved actions have been studied extensively [7,19–22], and it has been found that even on fairly coarse lattices (a up to 0.4 fm) good results can be obtained for hadron masses by estimating the coefficients of the improvement terms using tadpole-improved perturbation theory. For the energy differences that we measure, we find that the improved action works very well. There are no signs of lattice-spacing dependence at a up to 0.4 fm, so as well as greatly reducing the computer resources required, it enables us to dispense with the extrapolation in a that is usually needed to obtain continuum results.

Our lattice glue and quark action parameters are summarized in table I and are described in detail in Ref. [7]. For the glue we use a Lüscher-Weisz (plaquette and 2×1 rectangle) action [20,21]. We measured the lattice spacing by NRQCD calculations of the charmonium $P-S$ splitting, using the experimental spin-averaged value of 458 MeV.

For the quarks we use a D234 action, which includes third and fourth derivative terms as well as an improved clover term. All the coefficients in the action are evaluated at tree level in tadpole-improved perturbation theory [23], using the mean link in Landau gauge to estimate the tadpole contribution. We work at a quark mass close to the physical strange quark: the pseudoscalar to vector meson mass ratio m_P/m_V is 0.76.

We collected data at two lattice spacings, $a = 0.40$ and 0.25 fm. The scaling of the hadron masses is good but not perfect: the pseudoscalar weighed 790 MeV on our coarser lattice and 840 MeV on the finer one. For our fits to eq. (1) in Sect. IV we used the average.

C. Sources and fitting

To look for bound $0^{++} \bar{q}^2 q^2$ states, we investigate states of two pseudoscalar mesons on lattices of various volumes, keeping only quark-line-connected diagrams. We calculate the binding energy δE_E in the exotic channel (flavor states that are only possible for a $\bar{q}^2 q^2$ state, ie $I = 2$ for two flavors, the **27** for three flavors) and the binding energy δE_N in the non-exotic channel (flavor states that could be $\bar{q}^2 q^2$ or $\bar{q}q$, ie $I = 0$ for two flavors, the **8** and **1** for three flavors). We could have used sources based on preconceptions about maximally attractive channels in QCD. For example, one-gluon exchange and instanton interactions are known to favor the color **3** diquark channel, leading to interesting phenomenology at high density [24], but we verified that these have good overlap with the two pseudoscalar meson source that we used.

Since we are interested in $\bar{q}^2 q^2$ states, we only study the D and C contributions. For each gauge field configuration we evaluate the pseudoscalar correlator $P(t)$ and the direct (“D”) and crossed (“C”) contributions to the two-pseudoscalar correlator. We use a wall source at $t = 0$, and both point and smeared sinks.

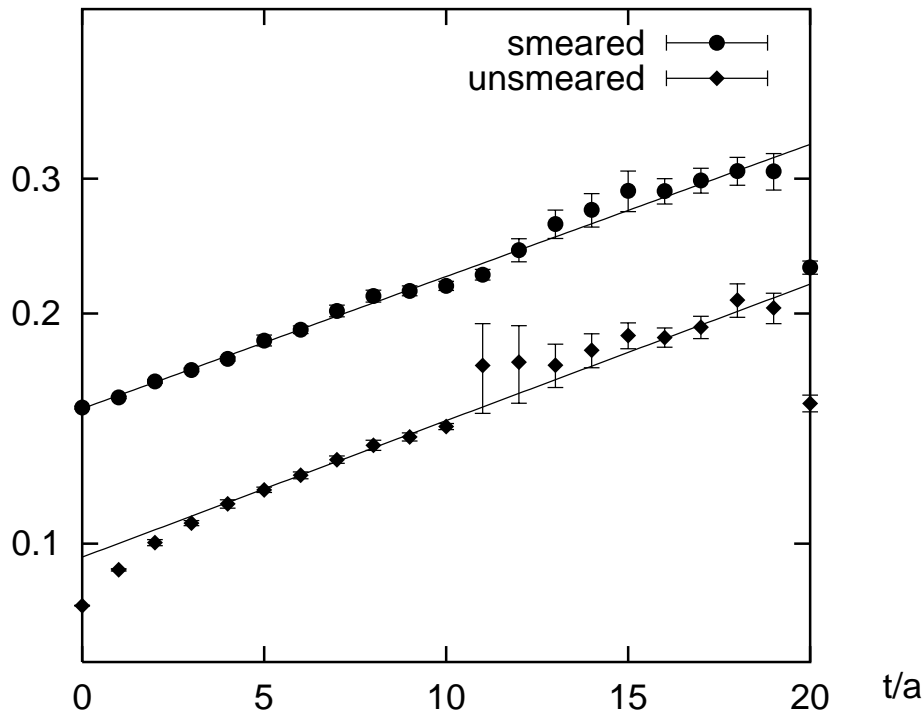


FIG. 4. Ratio of wall-source correlators $R_N(t)$ (see eq. (6)), on a log scale, for lattice spacing $a = 0.4$ fm, lattice size $L = 2$ fm. The lattice was 40 spacings (10 fm) long, but only the first half is shown. For the smeared data we fitted to an exponential using $t = 1$ to 17. For the unsmeared we used $t = 5$ to 17. The fitted values of δE_N agree.

$$\begin{aligned}
 P(t) &= \sum_{\vec{x}} \text{Tr} \left(G(t, \vec{x}) G^\dagger(t, \vec{x}) \right) \\
 D(t) &= \sum_{\vec{x}} \left[\text{Tr} \left(G(t, \vec{x}) G^\dagger(t, \vec{x}) \right) \right]^2 \\
 C(t) &= \sum_{\vec{x}} \text{Tr} \left(G(t, \vec{x}) G^\dagger(t, \vec{x}) G(t, \vec{x}) G^\dagger(t, \vec{x}) \right)
 \end{aligned} \tag{4}$$

where the trace is over color and spinor indices, and $G(t, \vec{x})$ is the quark propagator in a given gauge background from a wall source at $t = 0$ to the point \vec{x} at time t . For smeared correlators, we performed covariant smearing at the sink. Note that the source for a pseudoscalar meson is $\bar{\psi}\gamma_5\psi$, and the inverse propagator $G^{-1}(t, \vec{x}) = \gamma_5 G(t, \vec{x}) \gamma_5$, so no factors of γ_5 appear in eq. (4).

We construct the exotic and non-exotic correlators

$$\begin{aligned}
 J_N(t) &= \langle D(t) \rangle + \frac{1}{2} \langle C(t) \rangle \\
 J_E(t) &= \langle D(t) \rangle - \langle C(t) \rangle,
 \end{aligned} \tag{5}$$

where the angle brackets signify an average over the ensemble of gauge field configurations.

To obtain the binding energy δE_N in the $I = 0$ channel, and the binding energy δE_E in the $I = 2$ channel, we construct ratios of correlators and fit them to an exponential

group	β	a^{-1} (MeV)	κ	m_P/m_V	m_P (MeV)
Gupta et al. [5]	Wilson 6.0	2590(60) [25]	0.154	—	940(30)
Fukugita et al. [6]	Wilson 5.7	1220(180) [25]	0.164	0.740(8)	620(90)
this work	L&W 1.719	790(10) [7]	—	0.756(5)	840(11)
	L&W 1.157	495(4) [7]	—	0.756(4)	790(6)

TABLE I. Lattice parameters for studies of P - P scattering states. Lattice spacings are determined by charmonium or upilon P - S splitting

$$\begin{aligned}
R_N(t) &= \frac{J_N(t)}{\langle P(t) \rangle^2} \sim A \exp(-\delta E_N t), \\
R_E(t) &= \frac{J_E(t)}{\langle P(t) \rangle^2} \sim B \exp(-\delta E_E t).
\end{aligned}
\tag{6}$$

The ratios of correlators are expected to take the single exponential form only at large t , after contributions from excited states have died away. We followed the usual procedure of looking for a plateau, and checking that smeared and unsmeared correlators give consistent results. The results for a typical case are shown in Fig. 4. There is no difficulty in identifying the plateau and extracting δE_N .

IV. RESULTS AND DISCUSSION

A. Our Results

We measured δE_N and δE_E for several different lattice spacings and sizes. Our results are shown in Fig. 5 along with previous results from Refs. [5,6]. The exotic and non-exotic channels appear to scale differently as a function of L . The exotic channel falls like $1/L^3$, which is the expected form for a scattering state, eq. (1). A fit is given in Table II, and shown in the figure. The non-exotic channel appears to depart from $1/L^3$ falloff. To be complete, however, we have fitted the non-exotic data also to the form expected for a scattering state. The results are given in Table II and in the figure.

The parameters of the lattice calculations are given in Table I. The lattice spacings were determined by quarkonium P - S splittings, using either charmonium or upilon experimental measurements to set the scale.

Although we only studied one quark mass, Gupta et al. [5] repeated their calculation for a lower quark mass, corresponding to $m_P = 770$ MeV, and found that δE_N and δE_E were unchanged to within statistical errors. This suggests that studies of $\bar{q}^2 q^2$ operators near $\bar{q}q$ - $\bar{q}q$ thresholds are not too sensitive to quark masses and leads us to combine the energy splittings from the different calculations in Table I on the same plot. For the δE_E data we display both Gupta et al. and Fukugita et al.'s results with our own. We enlarged the error bar on Fukugita et al.'s point to 14%, since Ref. [25] quoted a 14% uncertainty in measuring their lattice spacing, which arises from the discretization errors involved in using an unimproved action on a coarse lattice. These are also apparent from the fact that Ref [6]'s m_P/m_V is close to ours, but its m_P is significantly lower. For δE_N we do not use

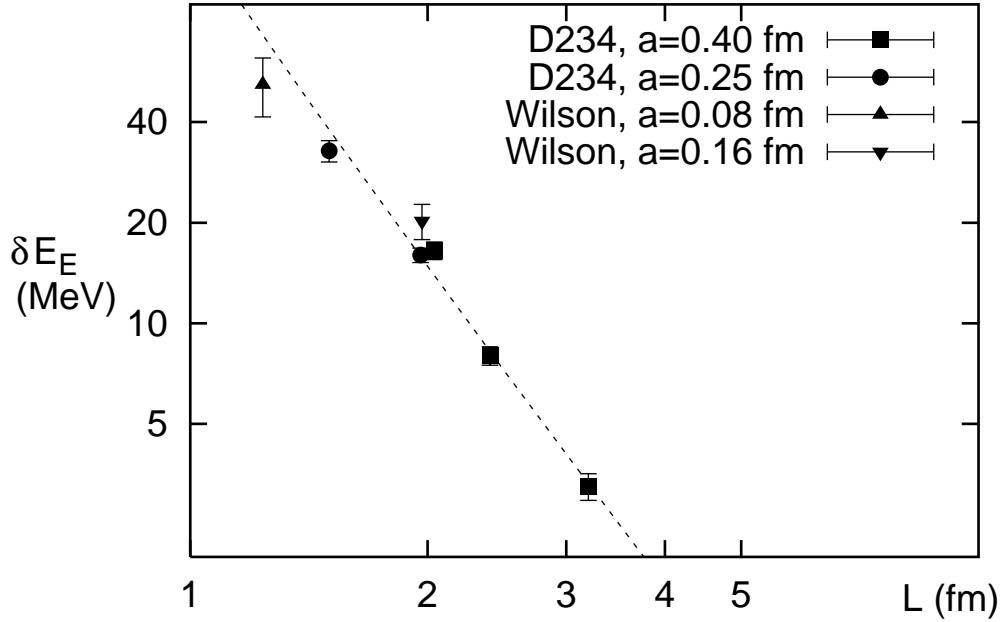
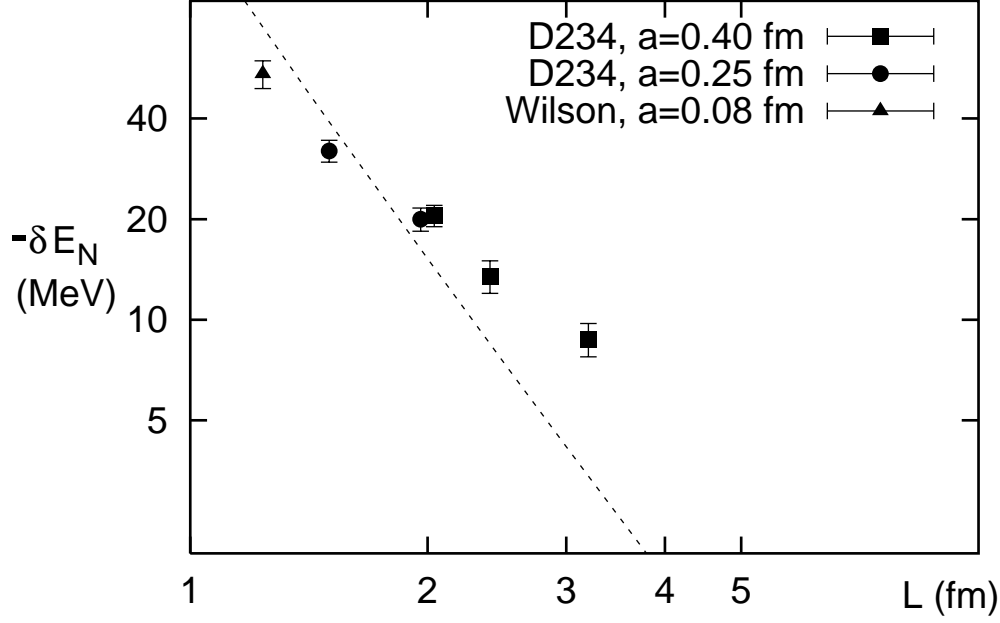


FIG. 5. P - P binding energy in non-exotic (N) and exotic (E) channels. The data at $a = 0.08$ fm are from [5]; the data at $a = 0.16$ fm are from [6]. The $a = 0.25$ fm and $a = 0.4$ fm points at $L = 2$ fm have been displaced slightly to either side in order to distinguish them. The lines are fits to eq. (1) (see table II).

channel	amplitude $T(\text{MeV}^{-2})$	χ^2/dof	dof	$4f_P^2 T$
non-exotic	$1.20(5) \times 10^{-5}$	17.0	5	—
exotic	$1.18(3) \times 10^{-5}$	3.0	6	1.03(3)

TABLE II. Threshold scattering amplitudes T obtained by fitting lattice calculations of δE_N and δE_E to the scattering-state form eq. (1). In the chiral limit, $4f_\pi^2 T = 1$. The non-exotic channel data does not fit the scattering-state form, so its fitted T is meaningless.

Fukugita et al.’s data, since they included the annihilation diagrams, which we specifically exclude in order to see a $\bar{q}^2 q^2$ state.

Our results are consistent with those of Refs. [5,6], even though we use much coarser lattices. This supports our use of Symanzik-improved glue and quark actions with tadpole-improved coefficients. As a further check on the validity of the improved actions, we note that at $L = 2$ fm, where we performed a calculation at two different lattice spacings for the same lattice volume, the results for the two lattice spacings agree very well. There is no evidence of any discretization errors.

For the exotic $\bar{q}^2 q^2$ system, the fit to eq. (1) is quite good, and the fitted scattering amplitude is remarkably similar to the result expected in the chiral limit, $4f_P^2 T = 1$.³ We conclude that there are no surprises in the exotic channel – the interaction near threshold appears repulsive and the strength is close to that predicted by chiral perturbation theory.

The non-exotic $\bar{q}^2 q^2$ system, however, does not fit the expected scaling law at large L . The fit to eq. (1) has a very large χ^2 , and is so poor that the extracted amplitude T is meaningless. Instead δE_N appears to be approaching a negative constant at large L . Instead of a scattering state, we appear to be seeing a *bound state* in the non-exotic channel. Although our data are suggestive, they are not conclusive. It would be very interesting to gather more data at $L \gtrsim 4$ fm, as well as at a range of quark masses, in order to verify the existence of this new state in the quenched hadron spectrum.

B. Interpretation and Discussion

We have found evidence for a $\bar{q}^2 q^2$ bound state just below threshold in the non-exotic pseudoscalar-pseudoscalar s -wave. In 2-flavor QCD the bound state would correspond to an isosinglet meson coupling to $\pi\pi$. In 3-flavor QCD the non-exotic channel corresponds to an entire nonet including two non-strange isosinglets and an isotriplet, and two strange isodoublets (see Fig. 1b). We work with a large quark mass so our results are not directly applicable to $\pi\pi$ scattering, but they do resemble physical $K\bar{K}$ scattering.⁴ The known isosinglet $f_0(980)$ and isotriplet $a_0(980)$ mesons are obvious candidates to identify with the non-exotic $\bar{q}^2 q^2$ bound states we seem to have found on the lattice.

³Since we did not calculate f_P at our quark masses, we have used the value $f_P = 148$ MeV, derived from Ref. [5], Table 1.

⁴Although we work in the $SU(3)_f$ limit where all quark masses are equal.

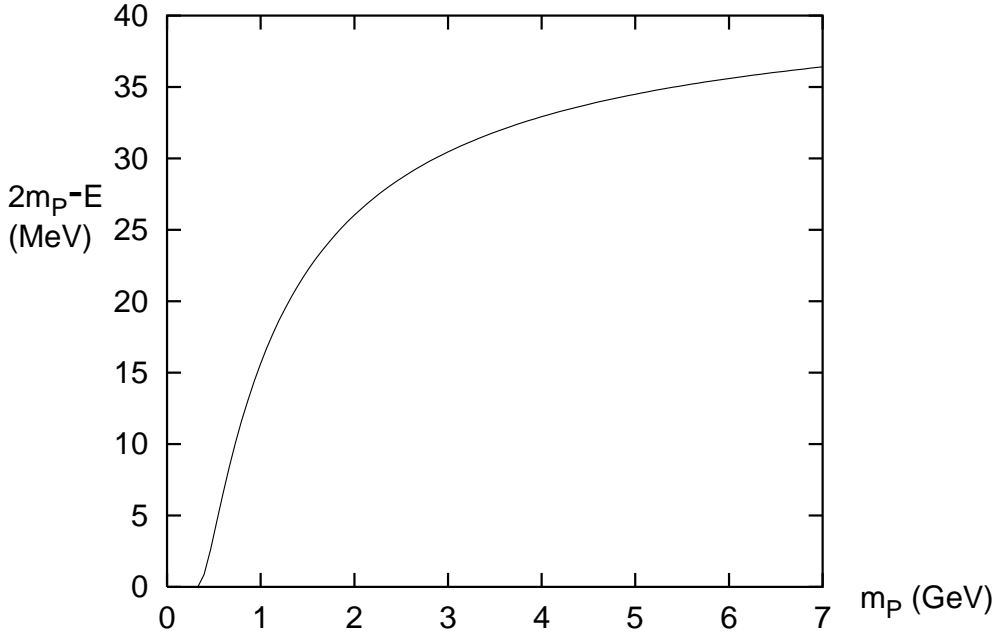


FIG. 6. Binding energy in MeV of the two-particle state in our toy model eq. (7), as a function of particle mass in GeV.

We believe the quark mass dependence of the non-exotic $\bar{q}^2 q^2$ state is quite different from a standard $\bar{q}q$ lattice state. In the quenched approximation the masses of $\bar{q}q$ states like those shown in Fig. 2 are roughly independent of m_P . Note especially that the masses are smooth as they cross the threshold, $2m_P$. In contrast, we believe that the $\bar{q}^2 q^2$ state we may have identified is strongly correlated with the PP threshold when the quark mass is large, and departs from it in a characteristic way as the quark mass is reduced. (Indirect support for this comes from Gupta et al.'s finding that their binding energy is independent of the pseudoscalar mass.) In particular, we believe that the bound state will move off into the meson-meson continuum as m_P is reduced toward the physical pion mass.

To explore the m_P dependence of our results, we have made a toy model based on a relativistic generalization of potential scattering. We write a Klein-Gordon equation for the s -wave relative meson-meson wavefunction, $\phi(r)$,

$$-\phi''(r) + (2m_P - U(r))^2 \phi(r) = E^2 \phi(r), \quad (7)$$

with the boundary condition that $\phi(0) = 0$. For $U(r) = 0$ the spectrum is a continuum beginning at $E = 2m_P$ as required. In the non-relativistic limit $m_P \ll |U|$, eq. (7) reduces to the Schrödinger equation with an attractive potential $-U(r)$ (for $U(r) > 0$). For sufficient depth and range, this potential will have a bound state. However, as $m_P \rightarrow 0$, the potential term in eq. (7) turns repulsive and the bound state disappears. Thus, if one keeps the depth and range of U fixed as one decreases m_P , the bound state moves out into the continuum and disappears. To be quantitative, we have taken a square well, $U(r) = U_0$, for $r \leq b$, and $U(r) = 0$ for $r > b$. We chose a range $b = 1/m_\pi \approx 1.4$ fm, and adjusted U_0 such that the bound state has binding energy of 10 MeV when $m_P \sim 800$ MeV. The bound state does indeed move off into the continuum (first as a virtual state) when m_P goes below 330 MeV.

The behavior of the bound state in this toy model is shown in Fig. 6. Note this toy model is not meant to be definitive⁵ but it illustrates the expected behavior of a P - P bound state: tracking $2m_P$ with roughly constant binding energy as m_P falls, then unbinding at some critical m_P .

On the basis of our lattice computation and the m_P dependence suggested by our toy model, we believe it is possible that *all* the phenomena associated with the light scalar mesons are linked to \bar{q}^2q^2 states. The narrow 0^{++} isosinglet $f_0(980)$ and isotriplet $a_0(980)$ mesons near $K\bar{K}$ threshold can be directly identified with \bar{q}^2q^2 lattice bound states (top line of Fig. 1b). The broad $\kappa(900)$ and $\sigma(600)$ (middle and bottom lines of Fig. 1b) couple to low mass ($\pi\pi$ or πK) channels. We speculate that they are to be identified as the continuum relics of the same objects which appear as bound states of heavy quarks.

Of course, a thorough examination of this question would require implementing flavor $SU(3)$ violation by giving the strange quark a larger mass. This would mix and split the isoscalars, shift the other multiplets (see Fig. 1b), and dramatically alter thresholds. For example, the $I = 1$ \bar{q}^2q^2 state couples both to $K\bar{K}$ and $\pi\eta$ (through the $\bar{s}s$ component of the η) in the quenched approximation. The fact that the physical $K\bar{K}$ and $\pi\eta$ thresholds are significantly different would certainly affect the manifestation of bound states such as those we have been discussing in the $SU(3)$ -flavor-symmetric limit.

C. Conclusions and Future Work

We have presented evidence for previously unknown pseudoscalar meson bound states in lattice QCD. Our results need confirmation. Calculations on larger lattices are needed, and variation with quark mass, lattice spacing, and discretization scheme should be explored.

In the real world a 0^{++} \bar{q}^2q^2 state may, depending on its flavor quantum numbers, mix with 0^{++} $\bar{q}q$ and glueball states. It seems natural to expect that for sufficiently heavy quarks a bound state will remain, but only full, unquenched lattice calculations can confirm this.

It is possible that an existing unquenched study of 0^{++} $\bar{q}q$ operators may show some corroboration of our results. In Ref. [13] the authors study $\bar{q}q$ sources with dynamical fermions. Although their interest was in exploring the mixing of 0^{++} $\bar{q}q$ with glueballs, there is nothing to stop their $\bar{q}q$ source from mixing with \bar{q}^2q^2 . So they should be sensitive to the \bar{q}^2q^2 bound state we have identified. It is therefore quite interesting that they report a 0^{++} state with an anomalously low mass ~ 800 MeV.

If light \bar{q}^2q^2 states are, in fact, a universal phenomenon, and if the $\sigma(600)$ is predominantly a \bar{q}^2q^2 object, then the chiral transformation properties of the σ have to be re-examined. The π and the $\sigma(600)$ are usually viewed as members of a (broken) chiral multiplet. In the naive $\bar{q}q$ model both π and σ are in the $(\frac{1}{2}, \frac{1}{2}) \oplus (\frac{1}{2}, \frac{1}{2})$ representation of $SU(2)_L \otimes SU(2)_R$ before symmetry breaking. In a \bar{q}^2q^2 model, as in the real world, the chiral transformation properties of the σ are not clear.

⁵ We could have chosen a different relativistic generalization of the Schrödinger equation which would have preserved the bound state as $m_P \rightarrow 0$. For example, we could have replaced $(2m_P - U)^2$ by $2m_P^2 - 2m_P U_1 - U_2^2$, and fine-tuned U_1 and U_2 to provide binding at arbitrarily low m_P .

If the phenomena that we have discussed survive the introduction of differing quark masses, then they will also have implications for heavy quark physics. For example, there could be a 0^{++} bound state just below the decay threshold for two D mesons in the charmonium spectrum.

Finally, we note that calculations similar to ours could be undertaken in the meson-baryon sector and in other J^{PC} meson channels. It has long been speculated that the $\Lambda(1405)$ is some sort of KN bound state [26] and $\bar{q}^2 q^2$ states have been postulated in other meson-meson partial waves.

V. ACKNOWLEDGMENTS

We would like to thank the members of the CTP Phenomenology Club for the stimulating environment in which this project was conceived, and Craig McNeile, Weonjong Lee, and Seyong Kim for discussions of their published work.

This work is supported in part by funds provided by the U.S. Department of Energy (D.O.E.) under cooperative research agreement #DF-FC02-94ER40818. The lattice QCD calculations were performed on the SP-2 at the Cornell Theory Center, which receives funding from Cornell University, New York State, federal agencies, and corporate partners. The code was written by P. Lepage, T. Klassen, and M. Alford.

REFERENCES

- [1] For a discussion with references, see the mini-review in C. Caso et al., *Eur. Phys. J.* **C3** (1998) 1.
- [2] D. Black, A. H. Fariborz, F. Sannino and J. Schechter, *Phys. Rev.* **D59** (1999) 074026.
- [3] R. Jaffe, *Phys. Rev.* **D15** (1977) 267.
- [4] J. Weinstein and N. Isgur, *Phys. Rev.* **D41** (1990) 2236.
- [5] R. Gupta, A. Patel, S. Sharpe, *Phys. Rev.* **D48** (1993) 388.
- [6] M. Fukugita et al., *Phys. Rev.* **D52** (1995) 3003.
- [7] M. Alford, T.R. Klassen, G.P. Lepage, *Phys. Rev.* **D58** (1998) 034503.
- [8] H. Hamber, E. Marinari, G. Parisi, C. Rebbi, *Nucl. Phys.* **B225** (1983) 475; M. Lüscher, *Commun. Math. Phys.* **104** (1986) 177; **105** (1986) 153; *Nucl. Phys.* **B354** (1991) 531.
- [9] S. Weinberg, *Phys. Rev. Lett.* **17** (1966) 616.
- [10] N. A. Tornqvist and M. Roos, *Phys. Rev. Lett.* **76** (1996) 1575.
- [11] R. Jaffe and F. E. Low, *Phys. Rev.* **D19** (1979) 2105.
- [12] G. Bali et al., *Nucl. Phys. Proc. Suppl.* **63** (1998) 209.
- [13] C. Michael, M. Foster, C. McNeile, [hep-lat/9909036](#).
- [14] W. Lee and D. Weingarten, [hep-lat/9910008](#).
- [15] S. Kim and S. Ohta, *Nucl. Phys. Proc. Suppl.* **63** (1998) 185.
- [16] P. Lacey et al., *Phys. Rev.* **D54** (1996) 6997.
- [17] M. Göckeler et al., *Phys. Rev.* **D57** (1998) 5562.
- [18] R. Gupta, A. Patel, S. Sharpe, *Nucl. Phys.* **B383** (1992) 309.
- [19] P. Weisz and R. Wohlert, *Nucl. Phys.* **B236** (1984) 397, erratum **B247** (1984) 544.
- [20] M. Lüscher and P. Weisz, *Comm. Math. Phys.* **97** (1985) 59, erratum **98** (1985) 433.
- [21] M. Alford, W. Dimm, G.P. Lepage, G. Hockney, P.B. Mackenzie, *Phys. Lett.* **B361** (1995) 87.
- [22] M. Alford, T.R. Klassen, G.P. Lepage, *Nucl. Phys.* **B496** (1997) 377.
- [23] G.P. Lepage and P.B. Mackenzie, *Phys. Rev.* **D48** (1993) 2250.
- [24] M. Alford, K. Rajagopal and F. Wilczek, *Phys. Lett.* **B422** (1998) 247, *Nucl. Phys.* **B537** (1999) 443; R. Rapp, T. Schäfer, E. V. Shuryak and M. Velkovsky, *Phys. Rev. Lett.* **81** (1998) 53;
- [25] C.T.H. Davies et al., *Phys. Rev.* **D56** (1997) 2755.
- [26] S. Pakvasa and S. F. Tuan, *Phys. Lett.* **B459** (1999) 301.